MRS Communications (2012), *2*, 85–89
© Materials Research Society, 2012
doi:10.1557/mrc.2012.13

MRS Communications

Research Letters

In situ small-angle x-ray scattering analysis of improved catalyst—support interactions through nitrogen modification

Kevin N. Wood, Department of Metallurgical & Materials Engineering, Colorado School of Mines, Golden, Colorado 80401
Steven T. Christensen, National Renewable Energy Laboratory, Golden, Colorado 80401
Svitlana Pylypenko, Department of Metallurgical & Materials Engineering, Colorado School of Mines, Golden, Colorado 80401
Tim S. Olson, National Renewable Energy Laboratory, Golden, Colorado 80401
Arrelaine A. Dameron, National Renewable Energy Laboratory, Golden, Colorado 80401
Katherine E. Hurst, Huyen N. Dinh, and **Thomas Gennett,** National Renewable Energy Laboratory, Golden, Colorado 80401
Ryan O'Hayre, Department of Metallurgical & Materials Engineering, Colorado School of Mines, Golden, Colorado 80401

Address all correspondence to Ryan O'Hayre at **rohayre@mines.edu**

(Received 9 April 2012; accepted 20 June 2012)

Abstract

In situ small-angle x-ray scattering (SAXS) is used to investigate the electrochemical durability of Pt-Metal (Pt-M) catalysts sputtered onto nitrogen-modified high surface area carbon powder. The results demonstrate that nitrogen modification promotes catalyst durability through reduction of nanoparticle dissolution and coarsening. Although particle sizes of Pt-M on high surface area carbon supports can be difficult to determine with transmission electron microscopy (TEM), a novel SAXS method has been employed to calculate particle size. SAXS analysis shows that the Pt-M nanoparticle size distribution remained stable for 3000 electrochemical cycles after nitrogen modification, whereas the unmodified support material leads to Pt-M nanoparticle instabilities. These results for industrial-relevant catalyst/support architectures underscore the potential of nitrogen-modified carbon support structures for enhanced Pt-M catalyst durability.

Heterogeneous catalysts often employ nanostructured materials that are susceptible to deleterious morphological changes during operation that reduce catalytic performance. Proton-exchange membrane fuel cells (PEMFCs) typically use high surface area carbon as a support material for metal nanoparticle catalysts. Despite the many advances in PEMFC technology over the past several decades, catalyst durability is still one of the key hurdles preventing large-scale PEMFC commercialization. This major issue is one of the main causes for degradation in fuel cell performance and is prevalent in both Pt and Pt-M (M = Ru, Co, Ni, etc.) catalysts.[1]

Catalyst degradation over time results in a loss of current due to several possible effects, including (i) changes in the alloy composition and arrangement of the M atoms on the surface, (ii) particle agglomeration via migration and coalescence or modified Ostwald ripening and (iii) Pt and M atom dissolution. These effects have led to considerable research focus on the development of support materials that will improve catalyst durability.[2–5]

Recently, many groups have indicated that nitrogen functionalities are complicit in modifying the nucleation and growth of nano-catalysts.[6–8] Similarly, it has also been hypothesized that these nitrogen groups enhance the binding of catalyst to support.[9–12] These results have been demonstrated theoretically; however, so far they have only been experimentally quantified using simplified model catalyst/support systems.[12–16] Here, we show a clear increase in Pt-M nano-catalyst durability on a commercially relevant, high surface area nitrogen-modified carbon powder when compared with an otherwise identical unmodified control powder. Furthermore, these results also confirm the role of nitrogen in modifying the nucleation and growth of Pt-M nano-catalysts. In this work we report results obtained using in situ SAXS analysis during accelerated electrochemical durability testing.

Powder catalyst samples were fabricated in a custom sputter chamber[17] using a combination of ion implantation and sputtering. During an experiment a standard mass (500 mg) of commercially available carbon powder (Cabbot Vulcan XCR72R) was put into a rotating sample holder (rotating wheel), and the chamber was evacuated to less than 5×10^{-6} Torr. Prior to any implantation or sputtering the carbon powders were out-gassed by heating to above 180 °C for 15 min. Nitrogen-modified samples were fabricated by ion implantation, prior to sputtering, at a pressure of 1×10^{-3} Torr (N_2) using a 20 mA beam current, 55 V discharge voltage and 100 V acceleration voltage for 90 min. XPS data contained in the Supplementary information shows the increase in atomic concentration of nitrogen. The metal catalyst was introduced

https://doi.org/10.1557/mrc.2012.13 Published online by Cambridge University Press

onto both unmodified and nitrogen-modified, out-gassed samples by sputtering from an alloyed $Pt_{0.50}Ru_{0.50}$ target at 25 mTorr with 10 mol% O_2:Ar at 45 W DC for 60 min.[17]

The electrodes were prepared by applying catalyst ink drop wise to SGL Carbon 25BA gas diffusion backing. The inks were prepared to produce electrode catalyst layers with 1:1 carbon:Nafion ratios and total metal loadings of ~5 mg.

In situ small-angle x-ray scattering (SAXS) was conducted on beam line 1–4 (Fig. 1) of the Stanford Synchrotron Radiation Lightsource (SSRL) at SLAC National Accelerator Laboratory. Data were collected for 60 s at an incident photon energy of 8.33 keV using a Rayonix 165 CCD detector. For each electrode, data were collected every five electrochemical cycles for the first 100 cycles, and then every 100 cycles at the exact same location on the sample until the electrodes were cycled 3000 times. Each cycle was from 0 to 800 mV (versus reversible hydrogen electrode, RHE), at a sweep rate of 200 mV/s in 0.1 M perchloric acid (GSF Chemicals, Powell, OH) at room temperature. The cycling was completed in a custom electrochemical cell made of polyether ether ketone (PEEK), shown in Fig. 1(a). The x-ray path-length through the liquid was 0.5 mm less the 4 µm-thick prolene windows (Chemplex Industries, Palm City, FL). Examples of similar cells have been demonstrated elsewhere.[18,19]

These data were then analyzed with the Igor Pro (v. 6.22, Wavemetrics, Portland, OR) plug-in, Irena (v. 2.40). Collected experimental intensities are shown in Figs. 2(a) and 2(b). By subtracting the blank carbon backing data from the catalyst spectrum of interest, and normalizing the background noise, a proper comparison of the intensities could be made. This process was completed for each sample shown here. The intensities were then modeled using the following equation by means of the Irena software package for SAXS.[20]

$$I(Q) = |\Delta\rho|^2 \int_0^\infty |F(Q, r)|^2 V^2(r) NP(r) \mathrm{d}r, \qquad (1)$$

where Δρ is contrast, $F(Q, r)$ is scattering form factor, $V(r)$ is the particle volume, N is the total number of scattering particles, and $P(r)$ is the probability of occurrence of scattering site size r. In this experiment the probability was fit using a log-normal distribution, shown in (2), adopted from the NIST engineering statistics handbook:[21]

$$P(r) = \frac{1}{r - \mathrm{Min} * \mathrm{mean}\sqrt{2\pi}} e^{\frac{-ln\left(\frac{x-mean}{sdev}\right)^2}{2sdev^2}}. \qquad (2)$$

In this equation Min is the minimum diameter size, SD is the standard deviation of the size distribution, and mean is the mean diameter subtracted from the minimum particle size. Figures 2(c) and 2(d) show the results of the model fitting in terms of scattering diameters.

It has previously been shown that particle size and particle size distribution estimated by transmission electron microscopy

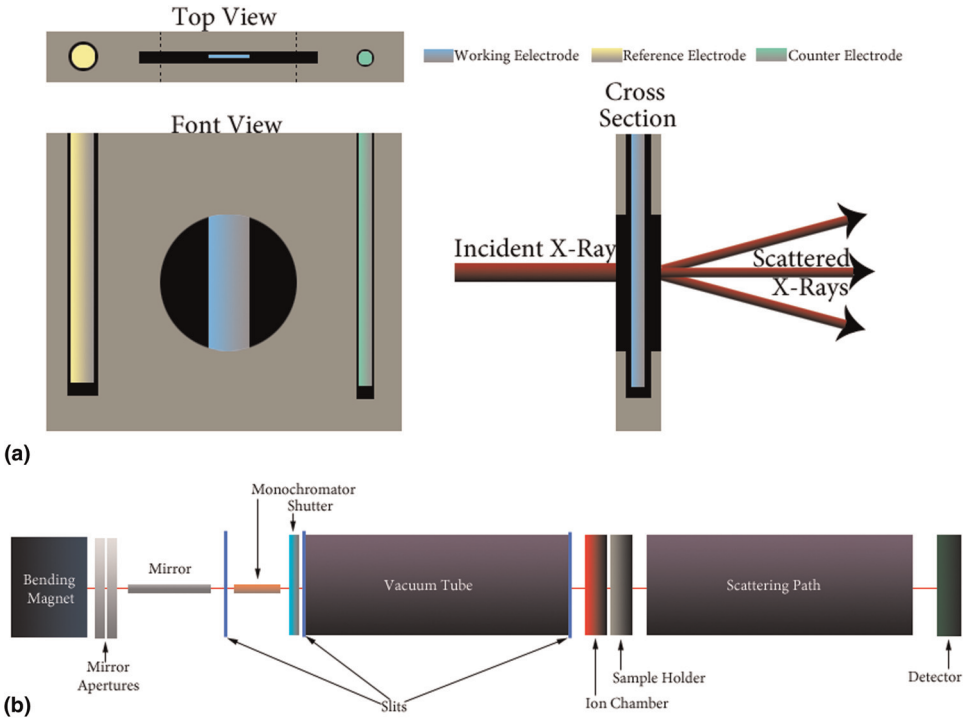


Figure 1. (a) The design of the in situ electrochemical cell allowing for analysis of the same precise area on the electrode. (b) A schematic of SLAC's beam line 1–4.

https://doi.org/10.1557/mrc.2012.13 Published online by Cambridge University Press

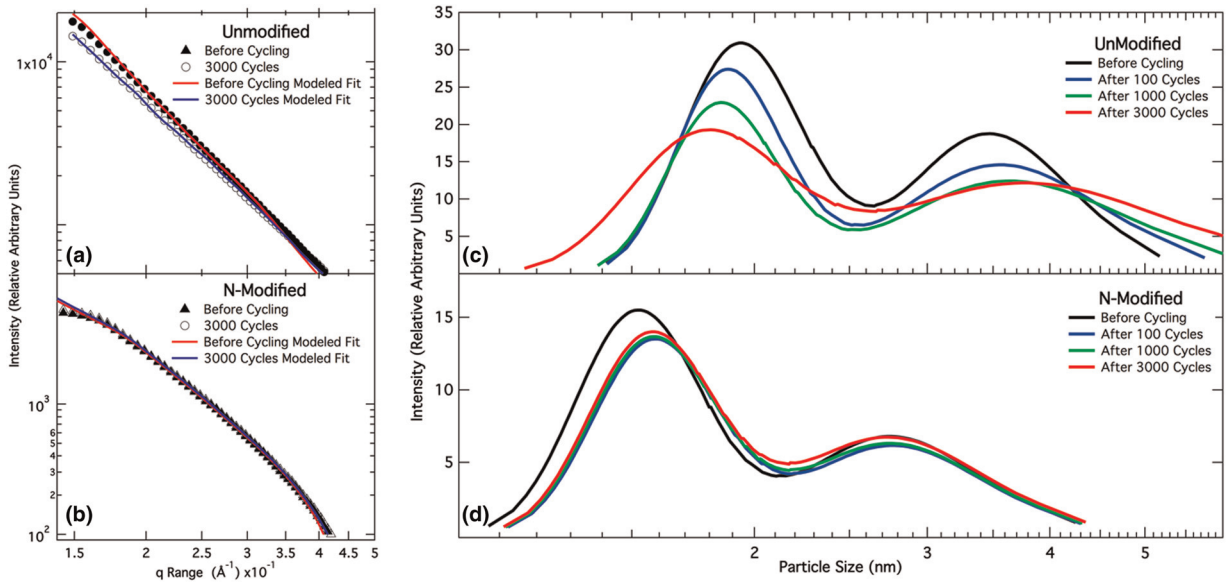


Figure 2. Modeled SAXS intensities shown with the collected experimental data for the unmodified (a) and nitrogen-modified (b) samples. The particle size distributions extracted from the SAXS modeling at various cycling times are shown in (c) and (d) for the unmodified and nitrogen-modified samples, respectively.

(TEM), x-ray diffraction (XRD), and SAXS closely match,[22,23] although TEM has been shown to sometimes overestimate particle size because measured particles can easily contain several primary crystallites.[23] As can be seen from the TEM images in Fig. 3, Pt-M nanoparticles obtained with sputtering have different morphologies from those obtained via other synthesis routes (i.e., colloidal deposition) and can have many nanoparticles located in close proximity to each other making estimation of the particle size challenging. Regions of less-dense particle coverage indicate particle sizes (~1–5 nm) within the range obtained by SAXS as shown in Fig. 3. SAXS also allows for better statistics because the spot size of the beam covers a larger, more comprehensive area, while particle size analysis using TEM is limited to small numbers of nanoparticles.

In Fig. 2(c), SAXS scattering diameters for the pre-cycled unmodified catalyst are shown. In general, the particle size distribution for this unmodified electrode shows a relatively wide bi-modal range of particles from ~1.8 to 5 nm in size. The particles can be roughly divided into two Gaussian distributions (as indicated on the plot): one distinct particle distribution at ~1.9 and another more broad distribution at 3.5 nm tailing toward higher particle sizes. After in situ accelerated degradation testing, the catalyst shows significant changes in particle size distribution, Fig. 2(c) (red line). The changes are most clearly seen in the increasing size and changing volume of the 5 nm size distribution, indicating the formation of large agglomerations. These agglomerates are likely caused by migration/coalescence and modified Ostwald ripening mechanisms. The leftward shift on the small particle size end of the distribution, which occurs simultaneously with the appearance of this peak change, is indicative of Ostwald ripening processes occurring through dissolution/reprecipitation.

For the nitrogen-modified support, Fig. 2(d) shows the initial particle distribution. Again two distinct particle sizes are observed; however, there are marked differences from the unmodified sample. The nitrogen-modified material shows a much narrower, more distinct and slightly smaller set of particle size distributions compared with the unmodified material (initial mean particle sizes are ~1.5 and 2.7 nm). The narrower widths and lower mean sizes associated with the bimodal Pt-M particle distribution on the nitrogen-modified carbon support are consistent with previous studies of Pt-M on carbon systems that show smaller average particle size and narrower particle size distributions for metal nanoparticles deposited on nitrogen-modified surfaces compared with unmodified surfaces.[24] These observations suggest that the nitrogen modification dramatically increases the ease of Pt-M nucleation on the carbon surface, thereby leading to smaller average particle size and a tighter particle size distribution.

After cycling, a small amount of particles near the 1.5 nm distribution was dissolved in-solution, but at a much slower rate than observed in the unmodified system. The absence of significant changes to the 2.7 nm particle size peak is important, indicating an improved binding interaction between the catalyst and support. Furthermore, most of the changes in the nitrogen-modified sample's particle distribution occurs in the first 100 electrochemical cycles, after which the distribution stabilizes and remains virtually unchanged out to 3000 cycles. This is in marked contrast to the unmodified sample, which shows significant continued changes in particle size distribution with increasing cycling, even out to 3000 cycles.

https://doi.org/10.1557/mrc.2012.13 Published online by Cambridge University Press

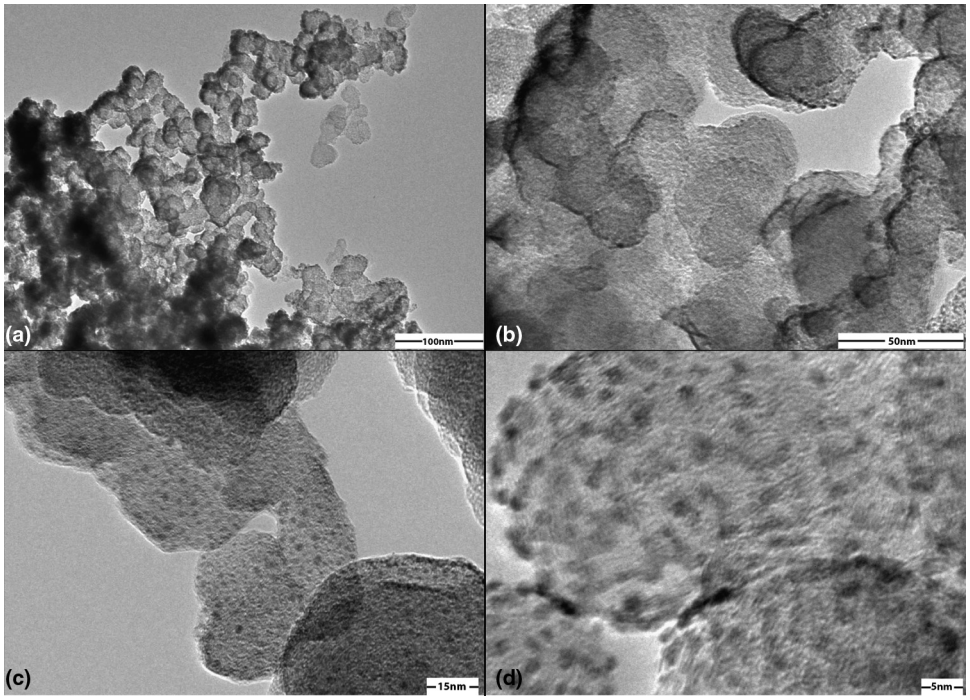


Figure 3. TEM images of the nitrogen-modified catalyst before cycling. (a, b) Low-magnification images demonstrating coverage of the sputtered PtRu/N-Carbon. Micrographs at higher magnification (c, d) show regions of less dense particle coverage demonstrating that nanoparticle size observed by TEM (~1–5 nm) is in agreement with values determined by SAXS.

These results suggest that nitrogen modification strongly mitigates the particle size growth observed in the unmodified sample, which facilitates significantly longer catalyst lifetime and increased catalyst performance over time due to the increased retention of catalyst surface area.

Conclusions

In this work we have compared the durability of Pt-M nanoparticle catalysts sputter deposited onto unmodified versus nitrogen-modified carbon supports via in situ (accelerated degradation testing) small-angle x-ray scattering. The results showed that nitrogen modification significantly increases the durability of the supported catalyst material over the course of an ADT protocol involving 3000 electrochemical cycles. This stabilization is achieved by a significant reduction in particle growth occurring through dissolution/redeposition and migration/coalescence processes on the support surface. The nitrogen modification also led to more desirable initial particle size distributions compared with the unmodified carbon support because of a more tightly distributed range of particle sizes in the optimal PEMFC catalyst size range between 1 and 4 nm. These results are of great significance in creating PEMFC catalysts with high durability. A full journal article containing electrochemical performance, SAXS, XRD and TEM is currently under preparation to further investigate the beneficial effect of nitrogen modified carbon supports.

Acknowledgments

This work was in cooperation with SLAC National Accelerator Laboratory. The work at CSM is supported by the Army Research Office under Grant No. W911NF-09-1-0528. The work at NREL is supported by the US Department of Energy EERE, FCT Program, under Contract No. DE-AC36-08-GO28308 with the National Renewable Energy Laboratory. The authors also acknowledge Electron Microscopy Laboratory at CSM.

Supplementary materials

For supplementary material for this article, please visit http://dx.doi.org/10.1557/mrc.2012.13

References

1. X. Xu and S. Ye: High-temperature fuel cell membranes based on mechanically stable para-ordered polybenzimidazole prepared by direct casting. *J. Power Sources* **172**, 145 (2007).
2. B. Shyam, T.M. Arruda, S. Murkjee, and D.E. Ramaker: Effect of RuO_xH_y island size on PtRu particle aging in methanol. *J. Phys. Chem.* C **113**, 19713 (2009).
3. B. Avasarala, R. Moore, and P. Haldar: Surface oxidation of carbon supports due to potential cycling under PEM fuel cell conditions. *Electrochim. Acta* **55**, 4765 (2010).
4. H.S. Choo, T. Kinumoto, S.K. Leong, Y. Iriyama, T. Abe, and Z. Ogumi: Mechanism for electrochemical oxidation of highly oriented pyrolytic graphite in sulfuric acid solution. *J. Electrochem. Soc.* **154**, B1017, (2007).
5. R. Borup, J. Meyers, B. Pivovar, Y.S. Kim, R. Mukundan, N. Garland, D. Myers, M. Wilson, F. Garzon, D. Wood, P. Zelenay, K. More,

https://doi.org/10.1557/mrc.2012.13 Published online by Cambridge University Press

K. Stroh, T. Zawodzinski, J. Boncella, J.E. McGrath, M. Inaba, K. Miyatake, M. Hori, K. Ota, Z. Ogumi, S. Miyata, A. Nishikata, Z. Siroma, Y. Uchimoto, K. Yasuda, K.I. Kimijima, and N. Iwashita: Scientific aspects of polymer electrolyte fuel cell durability and degradation. *Chemical Reviews*. **107**, 3904 (2007).
6. S. Ye, A.K. Vijh, and L.H. Dao: A new fuel cell electrocatalyst based on highly porous carbonized polyacrylonitrile foam with very low platinum loading. *J. Electrochem. Soc*. **143**, L7 (1996).
7. S.C. Roy, P.A. Christensen, A. Hamnett, K.M. Thomas, and V. Trapp: Direct methanol fuel cell cathodes with sulfur and nitrogen-based carbon functionality. *J. Electrochem. Soc*. **143**, 3073 (1996).
8. Y.K. Zhou, R. Pasquarelli, T. Holme, J. Berry, D. Ginley, and R. O'Hayre: Improving PEM fuel cell catalyst activity and durability using nitrogen-doped carbon supports: observations from model Pt/HOPG systems. *J. Mater. Chem*. **19**, 7830 (2009).
9. Y.G. Chen, J.J. Wang, H. Liu, R.Y. Li, X.L. Sun, S. Ye, and S. Knights: Enhanced stability of Pt electrocatalysts by nitrogen doping in CNTs for PEM fuel cells. *Electrochem. Commun*. **11**, 2071 (2009).
10. S. Maldonado and K.J. Stevenson: Influence of nitrogen doping on oxygen reduction electrocatalysis at carbon nanofiber electrodes. *J. Phys. Chem*. **B 109**, 4707 (2005).
11. S. Ye, K.A. Vijh, and L.H. Dao: A new fuel cell electrocatalyst based on carbonized polyacrylonitrile foam. *J. Electrochem. Soc*. **144**, 90 (1997).
12. T. Maiyalagan, B. Viswanathan, and U.V. Varadaraju: Nitrogen containing carbon nanotubes as supports for Pt – Alternate anodes for fuel cell applications. *Electrochem. Comm*. **7**, 905 (2005).
13. T. Holme, Y.K. Zhou, R. Pasquarelli, and R. O'Hayre: First principles study of doped carbon supports for enhanced platinum catalysts. *Phys. Chem. Chem. Phys*. **12**, 9461 (2010).
14. M.N. Groves, A.S.W. Chan, C. Malardier-Jugroot, and M. Jugroot: Improving platinum catalyst binding energy to graphene through nitrogen doping. *Chem. Phys. Lett*. **481**, 214 (2009).
15. S. Pylypenko, A. Queen, T.S. Olson, A. Dameron, K. O'Neill, K.C. Neyerlin, B. Pivovar, H.N. Dinh, D.S. Ginley, T. Gennett, and R. O'Hayre: Tuning carbon-based fuel cell catalyst support structures via nitrogen functionalization. I. Investigation of structural and compositional modification of highly oriented pyrolytic graphite model catalyst supports as a function of nitrogen implantation dose. *J. Phys. Chem*. C **115**, 13667 (2011).
16. S. Pylypenko, A. Queen, T.S. Olson, A. Dameron, K. O'Neill, K.C. Neyerlin, B. Pivovar, H.N. Dinh, D.S. Ginley, T. Gennett, and R. O'Hayre: Tuning carbon-based fuel cell catalyst support structures via nitrogen functionalization. II. Investigation of durability of Pt–Ru nanoparticles supported on highly oriented pyrolytic graphite model catalyst supports as a function of nitrogen implantation dose. *J. Phys. Chem*. C **115**, 13676 (2011).
17. A. Dameron, T.S. Olson, S.T. Christensen, J.E. Leisch, K.E. Hurst, S. Pylypenko, J.B. Bult, D.S. Ginley, R. O'Hayre, H.N. Dinh, and T. Gennett: Pt–Ru alloyed fuel cell catalysts sputtered from a single alloyed target. *ACS Catal*. **1**, 1307 (2011).
18. C. Yu, S. Koh, J. Leisch, M. Toney, and P. Strasser: Size and composition distribution dynamics of alloy nanoparticle electrocatalysts probed by anomalous small angle x-ray scattering (ASAXS). *Faraday Discuss*. **140**, 283 (2008).
19. C. Yu: Structural dynamics of Pt and Pt alloy nanoparticle probed by x-ray scattering techniques. Ph.D. Thesis, University of Houston, August 2010.
20. J. Ilavsky and P.R. Jemian: Irena: tool suite for modeling and analysis of small-angle scattering. *J. Appl. Crystallogr*. **42**, 347 (2009).
21. A.J. Allen, S. Krueger, G. Skandan, G.G. Long, H. Hahn, H.M. Kerch, J.C. Parker, and M.N. Ali: Microstructural evolution during the sintering of nanostructured ceramic oxides. *J. Am. Ceram. Soc*. **79**, 1201 (1996).
22. L.C. Gontard, R.E. Dunin-Borkowski, D. Ozkaya, T. Hyde, P.A. Midgley, and P. Ash: Crystal size and shape analysis of Pt nanoparticles in two and three dimensions. *J. Phys. Conf. Ser*. **26**, 367 (2006).
23. T. Hyde: Crystallite size analysis of supported platinum catalysts by XRD. *Platinum Met. Rev*. **52**, 129 (2008).
24. Y. Zhou, K. Neyerlin, T.S. Olson, S. Pylypenko, J. Bult, H.N. Dinh, T. Gennett, Z. Shao, and R. O'Hayre: Enhancement of Pt and Pt-alloy fuel cell catalyst activity and durability via nitrogen-modified carbon supports. *Energy Environ. Sci*. **3**, 1437 (2010).

https://doi.org/10.1557/mrc.2012.13 Published online by Cambridge University Press